Published in final edited form as:
Cell. 2008 October 31; 135(3): 549–560. doi:10.1016/j.cell.2008.09.060.

Neurofibromin regulation of ERK signaling modulates GABA release and learning

Yijun Cui[1], **Rui M Costa**[1,2], **Geoffrey G Murphy**[1,3], **Ype Elgersma**[1,4], **Yuan Zhu**[5], **David H. Gutmann**[6], **Luis F. Parada**[7], **Istvan Mody**[8], and **Alcino J Silva**[1]

[1]*Department of Neurobiology, Psychiatry, and Psychology, Brain Research Institute, University of California, Los Angeles, California 90095* [2]*Laboratory for Integrative Neuroscience, NIAAA, NIH, 5625 Fishers Lane, Room TS-20D, MSC 9411, Bethesda, Maryland 20852* [3]*Department of Molecular & Integrative Physiology, University of Michigan, Ann Arbor, Michigan 48109, USA* [4]*Erasmus MC, Dr. Molewaterplein 50, PO Box 2040, 3000 CA, Rotterdam, The Netherlands* [5]*Departments of Internal Medicine and Cell and Developmental Biology, University of Michigan Medical School, Ann Arbor, MI 48109.* [6]*Departments of Neurology, Washington University School of Medicine, St. Louis, MO 63110* [7]*Department of Developmental Biology, University of Texas Southwestern Medical Center, Dallas, Texas 75235, USA* [8]*Departments of Neurology and Physiology, University of California, Los Angeles, Los Angeles, California 90095*

Summary

We uncovered a new role for ERK signaling in GABA release, long-term potentiation (LTP) and learning, and show that disruption of this mechanism accounts for the learning deficits in a mouse model for Neurofibromatosis type I (NF1), a common genetic cause for learning disabilities. Genetic, pharmacological, electrophysiological and behavioral data demonstrate that neurofibromin modulates ERK/synapsin I dependent GABA release, which in turn modulate hippocampal LTP and learning. An *Nf1* heterozygous null mutation, which results in enhanced ERK and synapsin I phosphorylation, increased pre-synaptic GABA release in the hippocampus which was reversed by pharmacologically down-regulating ERK signaling. Importantly, the learning deficits associated with the *Nf1* mutation were rescued by a sub-threshold dose of a $GABA_A$ antagonist. Accordingly, Cre-deletions of the *Nf1* gene showed that only those deletions involving inhibitory neurons caused hippocampal inhibition, LTP and learning abnormalities. Importantly, our results also revealed lasting increases in GABA release triggered by learning, indicating that the mechanisms uncovered here are of general importance for learning and memory.

Introduction

Previous studies had implicated ERK signaling in learning and LTP, a synaptic plasticity mechanism thought to underlie learning & memory. This signaling pathway is activated during both LTP induction and learning, and decreases in its activity result in both LTP and learning deficits(Atkins et al., 1998; English and Sweatt, 1996, 1997; Selcher et al., 1999). ERK signaling is involved in a number of learning tasks, including associative fear conditioning (Atkins et al., 1998), spatial learning(Selcher et al., 1999), and conditioned place preference

Correspondence should be addressed to Dr. Alcino J. Silva, Departments of Neurobiology, Psychiatry, and Psychology, Brain Research Institute, University of California, Los Angeles, CA 90095. E-mail: E-mail: silvaa@mednet.ucla.edu.

(Gerdjikov et al., 2004). Likewise, ERK signaling in excitatory neurons is thought to modulate several forms of LTP(Chen et al., 2006; Kelleher et al., 2004; Kushner et al., 2005).

Neurofibromin, a Ras GPTase Activating Protein (RasGAP)encoded by the Neurofibromatosis Type I (NF1) gene(Martin et al., 1990; Xu et al., 1990) is thought to modulate Ras/ERK signaling, LTP and learning in mice(Costa et al., 2002; Li et al., 2005). The NF1 gene is expressed in neurons, Schwann cells, and oligodendrocytes as well as in many other non-neural cell types(Lynch and Gutmann, 2002). In patients, mutations of the NF1 gene cause learning disabilities and other cognitive symptoms(North, 2000). Visual-spatial problems are among the most common cognitive deficits detected in NF1 patients(Dilts et al., 1996). Interestingly, mice heterozygous for a null mutation of the *Nf1* gene ($Nf1^{+/-}$) also have spatial learning problems(Silva et al., 1997). Pharmacological or genetic approaches that reverse the enhancement in ERK signaling in $Nf1^{+/-}$-mice also reverse their LTP and spatial learning deficits(Costa et al., 2002; Li et al., 2005). However, these studies did not reveal how the increases in Ras/ERK signaling observed in the $Nf1^{+/-}$ mice led to changes in inhibition and deficits in LTP and learning. Here, we demonstrate a new role for ERK signaling in GABA release, LTP and learning, and show that disruption of this mechanism accounts for the learning deficits in an animal model of NF1. We show that the learning deficits of $Nf1^{+/-}$ mice are due to increases in ERK activation which lead to higher levels of synapsin I phosphorylation, greater GABA release and consequently to LTP and learning deficits.

Results

Neurofibromin in inhibitory neurons modulates learning

To investigate the mechanism responsible for the learning deficits associated with the $Nf1^{+/-}$ mutation, we tested learning in mice with heterozygous Cre-mediated deletions of the *Nf1* gene in key cell types in the brain. To generate lines with cell-type specific Cre-mediated deletions, we crossed a mouse line with the *Nf1* exons 31 and 32 flanked by lox P sites ($Nf1^{\text{floxed}}$)(Zhu et al., 2001) with mice expressing Cre-recombinase under the control of cell-type specific promoters: synapsin I promoter)(Zhu et al., 2001), GFAP promoter(Bajenaru et al., 2002), αCaMKII promoter(Chen et al., 2006), and Dlx5/6 promoter(Stenman et al., 2003). Therefore, the resulting mice included deletions of *Nf1* in the following cell types: both excitatory and inhibitory neurons ($Nf1^{syn\ I}$; with synapsin I-Cre), forebrain GABAergic neurons ($Nf1^{Dlx5/6}$; with Dlx5/6-cre), forebrain pyramidal neurons ($Nf1^{\alpha CaMKII}$; with αCaMKII-Cre), and astrocytes ($Nf1^{GFAP}$; with GFAP-Cre).

To confirm the Cre-mediated deletions, we performed Western blot analyses of neurofibromin levels in mice with homozygous Cre-mediated deletions. The results show that neurofibromin levels are reduced in the hippocampus (CA1 region) of the following mice with Cre-mediated homozygous deletions: $Nf1^{syn\ I-/-}$, $Nf1^{Dlx5/6-/-}$, and $Nf1^{\alpha CaMKII-/-}$ (Figure. S1). In contrast, The $Nf1^{GFAP-/-}$ mice do not show significant neurofibromin deletion (Figure. S1). However, detection of the *Nf1* deletion in these mice was difficult because the *Nf1* gene is expressed at low levels in astrocytes of adult mice(Zhu et al., 2001). It is important to note that not all GFAP-Cre lines show astrocyte-specific deletion (Zhuo et al., 2001). However, the line we used appears to restrict deletion to astrocytes(Hegedus et al., 2007). This could be due to the embryonic date when Cre is first expressed in these two lines(Hegedus et al., 2007).

NF1 patients have visual-spatial cognitive deficits(Dilts et al., 1996) and previous studies showed that the $Nf1^{+/-}$ mice have deficits in spatial learning (Morris water maze)(Silva et al., 1997), a task known to be sensitive to hippocampal lesions(Morris et al., 1982). Thus, the four lines of conditional mutants and controls were trained in the Morris water maze. As controls we used each of the Cre lines, heterozygous $Nf1^{floxed}$ ($Nf1^{floxed/+}$), as well as wild type (WT) mice. No differences were observed between the four conditional mutant lines and their

controls in performance on visible platform (Figure. S2), floating (continuous immobility for more than 10 sec during entire training), thigmotaxic behavior (swimming within 2 cm of pool wall; hug time during day 7 probe trial) or swimming speed during the day 7 probe trial (Table S1). Similarly, a comparison among all groups found no differences in the time taken to find the platform during training (Figure. S3). This is not surprising since this measure is known to be very insensitive to changes in spatial learning(Brandeis et al., 1989). After 7 days of training, the mice were tested in a probe trial, a very sensitive measure of spatial learning(D'Hooge and De Deyn, 2001; Lindner, 1997). The control lines (Table S2), as well as the $Nf1^{\alpha CaMKII+/-}$ and the $Nf1^{GFAP+/-}$ mice spent more time searching in the quadrant where the platform was during training (training quadrant) than in the other quadrants (Figure. 1 and Figure. S4). Surprisingly, even an ρCaMKII-Cre mediated homozygous deletion of *Nf1* ($Nf1^{\alpha CaMKII-/-}$) showed normal spatial learning (Figure. S5). In contrast, $Nf1^{syn\ I+/-}$ and the $Nf1^{Dlx5/6+/-}$ mice did not spend more time in the training quadrant than in other quadrants (Figure. 1 and Figure. S4). Accordingly, these two conditional mutant lines spent less time in the training quadrant than their controls (Table S3). These data demonstrate that heterozygous *Nf1* deletions driven by either synapsin I-Cre or Dlx5/6-Cre result in spatial learning deficits. Both of these lines are known to express Cre-recombinase in interneurons, an unexpected result suggesting a role for neurofibromin in inhibitory neurons.

Neurofibromin in inhibitory neurons modulates GABA release

Although previous results suggested that GABA-mediated inhibition is altered in $Nf1^{+/-}$ mice (Costa et al., 2002), the mechanisms were unknown. Therefore, we investigated next a possible role for neurofibromin in GABA-mediated inhibition. We examined both inhibitory and excitatory synaptic inputs to CA1pyramidal neurons in $Nf1^{+/-}$ mice. We first recorded spontaneous inhibitory postsynaptic currents (sIPSCs) in the present of kynurenic acid (1 mM) and miniature inhibitory postsynaptic currents (mIPSCs) in the presence of kynurenic acid (1 mM) and TTX (1μM). The sIPSCs and mIPSCs recorded from $Nf1^{+/-}$ and WT mice showed no difference in amplitude, frequency, rise time and decay time constant (Figure. 2a, 2b and Table S4), suggesting normal GABA-mediated inhibition under baseline conditions. However, there is evidence that during learning inhibitory neurons fire at high frequency (Nitz and McNaughton, 2004), and it is possible that under these conditions inhibition is altered in the $Nf1^{+/-}$ mice. Additionally, studies in excitatory neurons indicated that phosphorylation of an ERK site insynapsin I modulates release in response to high frequency stimulation(Chi et al., 2003), and a similar mechanism may also regulate release in inhibitory neurons.

Therefore, we compared the mIPSCs of $Nf1^{+/-}$ mice and controls after depolarization of synaptic terminals with high KCl (12.5 mM) in ACSF in the presence of kynurenic acid (1 mM) and TTX (1 μM) to mimic high frequency stimulation. These conditions did not change the relative mIPSC amplitude but resulted in a significant increase in mIPSC frequency in both WT and $Nf1^{+/-}$ mice (Figure. 2e). Importantly, the ratio between mIPSC frequency recorded in 12.5mM KCl versus that in control solution (2.5 mM KCl) was significantly larger in $Nf1^{+/-}$ mice than in their WT littermates (Figure. 2c), suggesting that under periods of high frequency stimulation neurofibromin regulates GABA release. It is important to note that both these electrophysiological results with $Nf1^{+/-}$ mice and our behavioral analysis of Cre-driven *Nf1* deletions indicate a role for neurofibromin in GABAergic neurons.

We also examined excitatory neurotransmission by recording miniature excitatory postsynaptic currents (mEPSCs), which result from spontaneous glutamate release by CA3 neurons on to CA1 neurons. We observed no significant differences in the properties of mEPSCs between the $Nf1^{+/-}$ mice and controls recorded with 2.5 mM KCl (Table S1). Depolarization of synaptic terminals with high KCl (12.5 mM) in ACSF increased the frequency of mEPSC in both WT and $Nf1^{+/-}$ neurons, but the ratio of mIPSC frequency

recorded in 12.5 mM KCl to that in control solution (2.5 mM KCl) was not significantly different between WT and $Nf1^{+/-}$ neurons (Figure 2d and 2f). Together with our behavioral analysis of Cre-driven deletion, this result indicates that heterozygous deletions of *Nf1* in excitatory neurons do not alter either synaptic function or learning.

The two *Nf1* heterozygous conditional mutant lines that showed spatial learning deficits, $Nf1^{syn\ I+/-}$ and $Nf1^{Dlx5/6+/-}$, also showed higher mIPSC frequencies (12.5 mM KCl). In contrast, the conditional lines that did not show behavioral deficits ($Nf1^{GFAP+/-}$ and $Nf1^{\alpha CaMKII+/-}$), also did not reveal changes in mIPSCs in either normal or 12.5 mM KCl ACSF (Figure 2g and 2h). These results demonstrate a critical role for neurofibromin (and by implication ERK signaling) in the regulation of GABA release from interneurons.

Neurofibromin regulates ERK-dependent GABA release

Neurofibromin is a RasGAP which accelerates the conversion of Ras from an active (GTP bound) to an inactive (GDP bound) state(Xu et al., 1990). Indeed, the $Nf1^{+/-}$ mutation leads to elevated Ras-GTP and hyper-activation of Ras downstream effectors such as ERK in the brain (Guilding et al., 2007; Li et al., 2005). To test if the increased GABA release we observed in $Nf1^{+/-}$ mice is caused by increased ERK signaling activity, we introduced MEK inhibitors U0126 and PD98095 to the perfusion ACSF bath solution to block the Ras-ERK signaling by inhibiting MEK, an ERK kinase. In ACSF with 12.5 mM KCl, introduction of U0126 reduced the frequency of mIPSCs in $Nf1^{+/-}$ mice to the levels of WTs (Figure. 3a). However, U0126 did not appreciably affect the mIPSCs frequencies of WT and $Nf1^{+/-}$ in 2.5 mM KCl ACSF. Similar results were also obtained with another MEK inhibitor, PD98095. Just as U0126, PD98095 did not affect the mIPSCs frequencies of WT and $Nf1^{+/-}$ with 2.5 mM KCl ACSF, but brought the frequency of mIPSCs in $Nf1^{+/-}$ mice to the levels of WTs measured in 12.5 mM KCl (Figure. 3b). Taken together, these results demonstrate a novel role for ERK signaling in the regulation of GABA release.

NF1 regulates learning- dependent synapsin I phosphorylation

Previous findings indicated that ERK phosphorylation of synapsin I modulates glutamate release under high frequency activation(Chi et al., 2003), and this could be also a mechanism for how neurofibromin regulates GABA release. Therefore, we characterized ERK activation and ERK-dependent phosphorylation of synapsin I in $Nf1^{+/-}$mice.

Immunohistochemistry studies in the CA1 region detected an increase in the number of ERK phosphorylation positive inhibitory neurons in both mutants and controls 30 min following 1-day training protocol in the water maze (5 trials). Also we found that the number of ERK phosphorylation positive inhibitory neurons was overall higher in $Nf1^{+/-}$ mutants than in controls (Figure. 4e and 4f). However, due to the difficulties in quantitating immunocitochemistry data, we next carried out western analysis studies.

We decided to use fear conditioning instead of water maze because this one-trial learning task is known to engage hippocampal function and result in the phosphorylation of both ERK and synapsin I(Atkins et al., 1998; Kushner et al., 2005). Unlike the water maze paradigms we used, where learning is distributed through multiple trials taking nearly an hour, in this task learning is concentrated on a single session lasting only 5 min. This allows for better synchronization of learning processes and therefore phosphorylation signals that are more robust and homogeneous. Hippocampal lysates were prepared from $Nf1^{+/-}$ and WT littermates after contextual fear conditioning training. To characterize ERK activation and ERK-dependent phosphorylation of synapsin I in $Nf1^{+/-}$ mutants, mice were trained with a paradigm known to trigger biochemical changes related to conditioning(Kushner et al., 2005) (three foot-shocks, each consisting of 0.75 mA for 2 sec, that were delivered with a 58-sec inter-shock

interval after being placed in a conditioning chamber for 2 minutes). This strong training paradigm is ideally suited to trigger robust biochemical changes in the hippocampus(Atkins et al., 1998; Kushner et al., 2005), but results in ceiling-level freezing responses that occlude conditioning differences between the genotypes (data not shown). However, consistent with their hippocampal deficits, $Nf1^{+/-}$ mice showed significant impairments in this task when ceiling performances are avoided; $Nf1^{+/-}$ mice and WT controls were given one trial/day for 5 days and their freezing responses were measured for 30 seconds on each training day and 24 hours after the last training trial. (Figure. 4a). Contextual conditioning significantly increased phosphorylation of both ERK and synapsin I (at the ERK site) in WT and $Nf1^{+/-}$ mice. Importantly, the increase in ERK phosphorylation in $Nf1^{+/-}$ mice is higher than in WT controls (Figure. 4b, 4c and Figure. S6). As a control, we also used a training procedure that does not trigger contextual learning (Fanselow, 1986) in which the footshock is administered immediately after introducing animals to the training context (immediate shock). This procedure did not cause an increase in ERK phosphorylation in either $Nf1^{+/-}$ or WT mice (data not shown), a resulting attesting to the learning specificity of ERK phosphorylation triggered with contextual conditioning (e.g. not caused by footshock). Similarly, $Nf1^{+/-}$ mice showed higher synapsin I phosphorylation than WT controls (ERK-dependent sites 4/5; Figure. 4b, 4d and Figure. S6a and S6c). In contrast, synapsin I phosphorylation at the αCaMKII-dependent site 3 was equivalent in WT and $Nf1^{+/-}$ mice (data not shown). This result indicates that neurofibromin modulates ERK phosphorylation of synapsin I 4/5 sites during learning.

Importantly, the two *Nf1* heterozygous conditional mutant lines that showed spatial learning deficits, $Nf1^{syn\ I+/-}$ and $Nf1^{Dlx5/6+/-}$, showed higher ERK phosphorylation than WT controls (Figure. 4b and 4c). Consistently, $Nf1^{syn\ I+/-}$ and $Nf1^{Dlx5/6+/-}$ also showed higher phosphorylation of ERK-dependent sites 4/5 of synapsin I (Figure. 4b and 4d). These results demonstrate that neurofibromin specifically in inhibitory neurons regulates ERK signaling and synapsin I phosphorylation, a result that provides a mechanistic explanation for neurofibromin's role in GABA release.

Deletion of *Nf1* gene from inhibitory neurons leads to LTP deficits

Previous studies suggested that enhanced GABA-mediated inhibition in the $Nf1^{+/-}$ mice results in deficits in hippocampal LTP(Costa et al., 2002). Thus, we tested whether the Cre deletions that resulted in enhanced inhibition and learning deficits also caused deficits in LTP. Accordingly, we demonstrate that CA1 LTP triggered with a 5-theta burst tetanus was deficient in the $Nf1^{Dlx5/6+/-}$ mutants but not $Nf1^{\alpha CaMKII+/-}$ mutants. Between 40 and 50 min after the tetanus, the $Nf1^{Dlx5/6+/-}$ mice (n = 6 mice) showed 124.5% ±4.5% potentiation, the $Nf1^{\alpha CaMKII+/-}$ mice knockouts (n = 9 mice) showed 142.1%± 6.7% potentiation, whereas WT mice (n = 6 mice) showed 148.6% ±4.1% (Figure. 5) These results show that deleting *Nf1* specifically in inhibitory neurons leads to LTP deficits, confirming that the synaptic plasticity deficits of these mutants are caused by increases in inhibitory function.

The learning deficits of $Nf1^{+/-}$ mice can be reversed by decreasing GABA-mediated inhibition

The results described above suggest that the deletion of neurofibromin from inhibitory, but not astrocytes or excitatory neurons disrupt spatial leaning and memory. To test whether the learning deficits of these mice are due to enhancements in GABA-mediated inhibition, we used picrotoxin, a $GABA_A$ receptor antagonist. WT and $Nf1^{+/-}$ mice were injected intraperitoneally once a day for 3 days before the first training day, and then 30 min before daily training with either saline or 0.01 mg per Kg (body mass) picrotoxin. As before, mice were trained with two trials per day in the Morris water maze. Spatial memory was assessed in a probe trial (end of training day 7), in which the platform was removed from the pool and the mice were allowed to search for it for 60 s.

In all the experiments described next, no differences were observed between genotypes and/or treatments in acquisition, floating, thigmotaxic behavior or swimming speed (Supplemental Table S5 and Figure. S7). Analysis of the day 7 probe trial showed an interaction between genotype and treatment. Importantly, 0.01mg/Kg picrotoxin did not affect the searching time of WT mice in the training quadrant. However, $Nf1^{+/-}$ mice treated with 0.01mg/Kg picrotoxin searched significantly longer in the training quadrant than $Nf1^{+/-}$ mice treated with saline, and were indistinguishable from WT mice with or without treatment (Figure. 6). Importantly, a higher dose of picrotoxin (0.03mg/Kg) enhanced learning in both $Nf1^{+/-}$ mice and controls (Figure. S8). The finding that the learning deficits of $Nf1^{+/-}$ mice can be reversed with a dose of picrotoxin (0.01mg/Kg) that is ineffective in WT shows that these learning deficits can be rescued by decreased GABA-mediated inhibition. All together the results presented here demonstrate a new role for ERK signaling in GABA release and learning, and suggest a novel approach for treating the learning disabilities associated with NF1.

Spatial learning triggers lasting increases in GABA release

The results presented above suggest an unexpected link between GABA release and learning. To test whether spatial learning causes lasting changes in GABA release, C57BL/6N mice were first trained in the water maze. We included three groups: A *Learning group* which were given one day of spatial training, a *Swimming-only control group* that spent in average the same amount of time in the pool but got no spatial training, and a *Cage control group* that were never exposed to any aspect of handling or training. Sixty minutes after training mice were sacrificed and mIPSC (2.5 mM KCl) were studied as before (>1 hour slice incubations). Mice in the *Learning group* showed higher mIPSC frequency than either the *Swimming group* or the *Cage controls*(Figure 7). No differences were observed between the *Swimming group* and the *Cage controls*. In contrast with mIPSP frequency, the amplitude, rise time, and decay time constant were not significantly different between groups(Figure 7). These results indicate that spatial training causes a lasting (>2 hours) increase in GABA release in the hippocampal CA1 region.

Discussion

The results described here uncovered a new role for ERK signaling in GABA release, plasticity and learning. We also show that disruption of this mechanism accounts for the learning deficits associated with NF1. Our results demonstrate that the learning deficits in a mouse model of Neurofibromatosis type I are caused by increased hippocampal GABA-release which dampens hippocampal synaptic plasticity and consequently leads to hippocampal-dependent learning deficits. Importantly, we also showed that spatial learning triggers a lasting increase in GABA release, and demonstrate that neurofibromin modulates ERK-dependent phosphorylation of synapsin I and that this is critical for GABA release, LTP and learning. Thus, our findings suggest that the mechanisms uncovered in our NF1 studies are of general importance for learning and memory, and not just specific to the pathology of NF1.

A key finding reported here is that neurofibromin in inhibitory neurons regulates ERK dependent phosphorylation of synapsin I and consequently GABA release. First, we reported that $Nf1^{+/-}$ mice, as well as mice with either an *Nf1* deletion in inhibitory neurons ($Nf1^{Dlx5/6+/-}$) or in inhibitory and excitatory neurons ($Nf1^{Syn\ I+/-}$), showed increased frequency of mIPSCs a traditional marker of pre-synaptic effects, without changes in either mIPSC amplitude, rise time or decay constant, three common electrophysiological tags of post-synaptic changes in neurotransmission. In contrast, deletion of *Nf1* in excitatory neurons ($Nf1^{\alpha CaMKII+/-}$) or astrocytes ($Nf1^{GFAP+/-}$ did not affect mIPSCs. These results indicate that neurofibromin has a critical role in GABA release. Second, two different MEK inhibitors rescued the increase in mIPSC frequency observed in $Nf1^{+/-}$ mice, implicating the Ras/MEK/

ERK signaling pathway in GABA release. In addition, we showed that MEK inhibition, although less effectively, also affected mIPSC frequency in controls, indicating that these effects are not specific to *Nf1* mutants. However, importantly, the $Nf1^{+/-}$ mutation did not affect mEPSCs, indicating that neurofibromin does not modulate ERK's role in hippocampal glutamatergic release(Kushner et al., 2005). Previous work had indicated that the ERK signaling pathway modulates learning by regulating post-synaptic LTP mechanisms(Sweatt, 2004). Our results are not in contradiction with these earlier findings, and instead they suggest that other GAPs (Bernards and Settleman, 2004), control ERK signaling in excitatory neurons during learning.

How does neurofibromin/ERK signaling modulate GABA release? Previous reports implicated ERK signaling in synapsin I phosphorylation, vesicle docking and glutamate release under conditions of high stimulation frequency. Consistent with previous models of synapsin I function in excitatory neurons (Chi et al., 2003), our findings suggest that the higher ERK activation found in inhibitory neurons leads to higher levels of synapsin I phosphorylation and therefore to greater GABA release. We show that behavioral training known to engage the hippocampus(Frankland et al., 1998; Kim and Fanselow, 1992) results in more robust hippocampal ERK phosphorylation and ERK-dependent phosphorylation of synapsin I in *Nf1* mice, including those with the mutation restricted to inhibitory neurons ($Nf1^{Dlx5/6+/-}$). Since the deletion in $Nf1^{Dlx5/6+/-}$ is restricted to inhibitory neurons, we can attribute the increase in ERK and synapsin I phosphorylation to processes in these cells. Additionally, we showed that deletion of the *Nf1* gene in excitatory neurons does not affect either ERK, synapsin I phosphorylation or various measures of glutamate release, indicating that neurofibromin does not play a critical role in the modulation of ERK/synapsin I function in excitatory pre-synaptic terminals.

Importantly, mutations ($Nf1^{+/-}$, $Nf1^{Dlx5/6+/-}$ and $Nf1^{Syn\ I+/-}$) that affected GABA release also disrupted LTP, demonstrating that the LTP deficits previously reported for $Nf1^{+/-}$ mice are caused by increased GABA release. Additionally, the very same lines with increased hippocampal GABA release and LTP deficits also showed abnormal learning in a hippocampal-dependent task (i.e. Morris water maze), while the $Nf1^{\alpha CaMKII+/-}$ mice did not show either inhibition, LTP or learning abnormalities. Abnormally high levels of GABA released during learning, could result in increased hyperpolarization of excitatory neurons and consequently in deficits in LTP. In contrast, up-regulating ERK signaling pathway in excitatory neurons leads to enhancements of both LTP and learning in mice(Kushner et al., 2005), while down regulating it in excitatory neurons leads to LTP and learning deficits(Chen et al., 2006). Altogether these findings demonstrate that ERK signaling in both excitatory and inhibitory neurons is critical for synaptic plasticity and learning.

The results discussed above demonstrate that increases in GABA release can affect learning. But, does learning also affect GABA release? Our results demonstrate that spatial training in the Morris water maze caused a lasting increase in GABA release, a result consistent with the idea that changes in GABAergic function may have a role in orchestrating the circuit changes involved in memory. Although these findings suggest that learning normally involves increases in GABA release, our results demonstrate that the abnormally high GABA release documented for $Nf1^{+/-}$ mice disrupts LTP and learning.

Our findings also impact on the development of treatments for the learning disabilities associated with NF1; we demonstrated that increased GABA release is responsible for the LTP and learning deficits associated with $Nf1^{+/-}$ mice. This result is consistent with previous findings that GABAergic transmission is important in the regulation of synaptic plasticity and learning(Crestani et al., 2002; Introini-Collison et al., 1994; McElroy and Korol, 2005; Wiltgen et al., 2005). Based on our finding that *Nf1* mutants have increased inhibition, we were able to

reverse the learning deficits of the $Nf1^{+/-}$ mice with a dose of a $GABA_A$ antagonist (picrotoxin) that was shown not to enhance learning in WT mice. These results confirm the role of inhibition in the learning deficits associated with NF1 and suggest that safe strategies that decrease GABAmediated inhibition will be useful to treat the learning deficits associated with NF1. It is important to note that GABAergic drugs like picrotoxin have a limited clinical usefulness due to their dangerous convulsant properties. However, it may be possible to use safer GABAergic drugs that preserve the beneficial cognitive effects without the proconvulsant properties (Atack et al., 2006). Interestingly, a recent study also found that changes in GABA inhibition underlie the learning deficits of an animal model of Down syndrome(Kleschevnikov et al., 2004; Rueda et al., 2008) suggesting that GABA inhibition may have a prominent role in the pathophysiology of cognitive disorders.

Methods

Mouse breeding and genotyping

All animal protocols were approved by the Chancellor's Animal Research Committee of UCLA, and in accordance with the NIH guidelines. In this paper, we used 3–6 month old males and females. Studies with $Nf1^{+/-}$ mice were performed in 129T2/SvEmsJ-C57BL/6 F1 hybrids generated. WT littermates were used as controls. The mice with Cre-mediated deletions of the *Nf1* gene ($Nf1^{Dlx5/6+/-}$; $Nf1^{syn\ I+/-}$ $Nf1^{CamkII\ +/-}$; $Nf1^{GFAP+/-}$) were F1 progeny from a cross between the $Nf1^{floxed/+}$ and the cell-type specific Cre mice (*synapsin 1-Cre*, *GFAP-Cre*, *αCaMKII-Cre*, and *Dlx5/6-Cre*. The four lines with Cre-deletions of the *Nf1* gene (and their controls)were all in 129T2/SvEmsJ-C57BL/6 F1 hybrid genetic background. Since the 4 different $Nf1^{Cre+/-}$ lines share the same genetic background (all in 129T2/SvEmsJ-C57BL/6 F1 hybrids background), in some experiments we combined WT and $Nf1^{floxed/+}$ littermates of different conditional mutant lines. The $Nf1^{Cre-/-}$ mice were F2 progeny of the $Nf1^{Cre+/-}$ mice. Mice genotype were determined by PCR analysis of tail DNA samples as described before. All experiments were carried out with researchers blind to the genotype of the animals tested.

Western Blot Analysis

Immunoblot analyses were performed as described previously ((Elgersma et al., 2002). In Figure 4 and Figure 6S, tissue was collected 30 min after behavioral training. The primary antibodies used were against NF1 (1:300; Santa Cruz Biotechnology); phospho-ERK p42/p44 and total ERK p42/p44 (1:1,000; NEB); β-actin (1:5,000; Sigma); synapsin I (1:1000; NEB); phospho-synapsin I is a gift from P. Greengard (Rockefeller University, New York, NY). Blots were quantitated using ECL^+ and the Storm 860 phosphorimager system (Molecular Dynamics, Sunnyvale, CA).

Immunohistochemistry

Immunohistochemistry was performed using confocal microscopy as described previously (Kushner, et al. 2005). The primary antibodies used were against phospho-Thr202/Tyr204 ERK p42/p44 (New England Biolabs), GAD65/67 (Chemicon). FITC donkey anti-rabbit, cyanine 3 (Cy3) donkey anti-mouse were used as secondary antibodies. Sections were analyzed with a Zeiss LSM 510 confocal laser-scanning microscope using a 40× numerical aperture objective. Neuronal quantification was performed by counting cellular FITC fluorescence and cellular Cy3 immunofluorescence.

Behavioral analysis

The Morris water maze apparatus and procedures were previously described(Costa et al., 2002). Mice were trained with two trials per day for 7 d (30 sec ITI). Probe trials were administered after 5 and 7 d after the completion of training. For the studies that looked at

inhibition after water maze training, Mice were initially habituated for 7 days (2 mins handling and 5 mins swimming/day). Mice in the "*Learning group*" were spatial trained with 15 trials (5 min ITI). In each trial, mice were given 30 sec on a platform and another 60 sec to find the platform (Figure. S9). Two mice were excluded from further analysis because of floating. Mice in the "*Swimming-only group*" spent on average the same time as the "*Learning group*" in the pool, but no platform was present. To avoid fatigue, training was divided into 5 sessions (4 min each) with 15 min ITI. Mice in the "*Cage-control group*" were sacrificed immediately after removal from the home cage. Mice from both the "*Learning*" and "*Swimming-only*" groups were sacrificed 60 min after the last session, and mIPSCs (see below) were recorded. In the visible version of water maze, mice were trained to search for a marked platform that were placed at a different location for 5 trials during 1 day (30 min ITI).

The contextual fear conditioning apparatus was previously described(Anagnostaras et al., 2000). To avoid ceiling performances, mice were placed in a conditioning chamber for 40 sec after which they were given a foot-shock (0.40 mA, 2 sec). Mice were trained with one trial/day for 5 consecutive days. At each training day and 24 hours after the last training trial, the freezing levels were monitored for 30 seconds.

All values are reported as mean±SEM. A two-way ANOVA with repeated measures was used to analyze the acquisition data from the water maze and freezing levels in the fear conditioning. A single-factor ANOVA was used to analyze the performance in the water maze probe on the percentage time in quadrant. A paired t-test were used to analyze the proximity data and crossing time.

Electrophysiology

Transverse hippocampal slices (400 μm thick) were maintained in a submerged recording chamber perfused with artificial cerebrospinal fluid (ACSF) equilibrated with 95% O2 and 5% CO2 at 30°C. The ACSF contained the following (in mM): 120 NaCl, 2.5 KCl, 2.5 CaCl2, 1.3 MgSO4, 1.25 NaH2PO4, 26 NaHCO3, and 10 D-glucose. Field EPSPs (fEPSPs) were recorded with a metallic electrode in CA1 stratum radiatum. The Schaffer collaterals were stimulated with 100-sec test pulses via a bipolar electrode. The intensity of stimulation was fixed at 60 mA. LTP was induced by a 5-theta-burst tetanus stimulation protocol (each burst consists of four pulses at 100 Hz with a 200-msec interburst interval). Responses from the last 10-min block of recordings were compared using ANOVA was used with Fisher's PLSD for post hoc comparisons. Whole-cell voltage-clamp recordings(reference mody)(Hajos et al., 2000) using an Axopatch 200B amplifier (Axon Instruments, Foster City, CA) or a 3900A Integrating Patch Clamp Amplifier (Dagan, Minneapolis, MN) were performed to measure sIPSCs, mIPSCs and mEPSCs. All recordings were made from the soma of visually identified CA1 pyramidal neurons. Patch electrodes (3–8 M when filled) were filled with a solution containing (in mM): 140 CsCl, 4 NaCl, 1 MgCl2, 10 Hepes, 0.05 EGTA, 2 Mg-ATP, and 0.4 Mg-GTP. Whole-cell voltage-clamp recordings were performed at -60-70 mV. Series resistance was compensated to 75–80%. Only recordings during which series resistance changed less than 25% through the whole experiment were analyzed. All recordings were low-pass filtered at 2 kHz and on-line digitized at 10 kHz using a PCI-MIO 16E-4 data acquisition board (National Instruments, Austin, TX). sIPSCs, mIPSCs and mEPSCs were measured using an in-house data acquisition and analysis software(Hajos et al., 2000). Data are presented as mean ± SEM. Statistical comparisons of mEPSC data were performed using paired and unpaired t tests and ANOVA.

Supplementary Material

Refer to Web version on PubMed Central for supplementary material.

Acknowledgements

This work was supported by grants from the NIH (R01 NS38480), Neurofibromatosis Inc., the Children's Tumor Foundation and US Army (W81XWH-06-1-0174) to A.J.S. This work was also supported by a generous donation from C. M. Spivak to AJS. Y.C. was supported by a fellowship from the Children's Tumor Foundation. We thank P. Greengard and J. N. Jovanovic for the generous gift of the phospho-Syn I antibodies. We are grateful to Steven Kushner, Brandon M. Stell and Weizheng Wei for fruitful discussions.

Reference

Anagnostaras, SG.; Josselyn, SA.; Frankland, PW.; Silva, AJ. Learning & memory. Vol. 7. Cold Spring Harbor, NY: 2000. Computer-assisted behavioral assessment of Pavlovian fear conditioning in mice; p. 58-72.

Atack JR, Bayley PJ, Seabrook GR, Wafford KA, McKernan RM, Dawson GR. L-655,708 enhances cognition in rats but is not proconvulsant at a dose selective for alpha5-containing GABAA receptors. Neuropharmacology 2006;51:1023–1029. [PubMed: 17046030]

Atkins CM, Selcher JC, Petraitis JJ, Trzaskos JM, Sweatt JD. The MAPK cascade is required for mammalian associative learning. Nature neuroscience 1998;1:602–629.

Bajenaru ML, Zhu Y, Hedrick NM, Donahoe J, Parada LF, Gutmann DH. Astrocyte-specific inactivation of the neurofibromatosis 1 gene (NF1) is insufficient for astrocytoma formation. Molecular and cellular biology 2002;22:5100–5113. [PubMed: 12077339]

Bernards A, Settleman J. GAP control: regulating the regulators of small GTPases. Trends Cell Biol 2004;14:377–385. [PubMed: 15246431]

Brandeis R, Brandys Y, Yehuda S. The use of the Morris Water Maze in the study of memory and learning. Int J Neurosci 1989;48:29–69. [PubMed: 2684886]

Chen AP, Ohno M, Giese KP, Kuhn R, Chen RL, Silva AJ. Forebrain-specific knockout of B-raf kinase leads to deficits in hippocampal long-term potentiation, learning, and memory. Journal of neuroscience research 2006;83:28–38. [PubMed: 16342120]

Chi P, Greengard P, Ryan TA. Synaptic Vesicle Mobilization Is Regulated by Distinct Synapsin I Phosphorylation Pathways at Different Frequencies. Neuron 2003;38:69–78. [PubMed: 12691665]

Costa RM, Federov NB, Kogan JH, Murphy GG, Stern J, Ohno M, Kucherlapati R, Jacks T, Silva AJ. Mechanism for the learning deficits in a mouse model of neurofibromatosis type 1. Nature 2002;415:526–530. [PubMed: 11793011]

Crestani F, Keist R, Fritschy JM, Benke D, Vogt K, Prut L, Bluthmann H, Mohler H, Rudolph U. Trace fear conditioning involves hippocampal alpha5 GABA(A) receptors. Proc Natl Acad Sci U S A 2002;99:8980–8985. [PubMed: 12084936]

D'Hooge R, De Deyn PP. Applications of the Morris water maze in the study of learning and memory. Brain Research Reviews 2001;36:60–90. [PubMed: 11516773]

Dilts CV, Carey JC, Kircher JC, Hoffman RO, Creel D, Ward K, Clark E, Leonard CO. Children and adolescents with neurofibromatosis 1: a behavioral phenotype. J Dev Behav Pediatr 1996;17:229–239. [PubMed: 8856518]

Elgersma Y, Fedorov NB, Ikonen S, Choi ES, Elgersma M, Carvalho OM, Giese KP, Silva AJ. Inhibitory autophosphorylation of CaMKII controls PSD association, plasticity, and learning. Neuron 2002;36:493–505. [PubMed: 12408851]

English JD, Sweatt JD. Activation of p42 mitogen-activated protein kinase in hippocampal long term potentiation. The Journal of biological chemistry 1996;271:24329–24332. [PubMed: 8798683]

English JD, Sweatt JD. A requirement for the mitogen-activated protein kinase cascade in hippocampal long term potentiation. The Journal of biological chemistry 1997;272:19103–19106. [PubMed: 9235897]

Fanselow MS. Associative vs topographical accounts of the immediate shock-freezing deficit in rats: Implication for the response selection rules governing species-specific defensive reactions. Learning and Motivation 1986;7:16–39.

Frankland PW, Cestari V, Filipkowski RK, McDonald RJ, Silva AJ. The dorsal hippocampus is essential for context discrimination but not for contextual conditioning. Behavioral neuroscience 1998;112:863–874. [PubMed: 9733192]

Gerdjikov TV, Ross GM, Beninger RJ. Place preference induced by nucleus accumbens amphetamine is impaired by antagonists of ERK or p38 MAP kinases in rats. Behavioral neuroscience 2004;118:740–750. [PubMed: 15301601]

Guilding C, McNair K, Stone TW, Morris BJ. Restored plasticity in a mouse model of neurofibromatosis type 1 via inhibition of hyperactive ERK and CREB. European Journal of Neuroscience 2007;25:99–105. [PubMed: 17241271]

Hajos N, Nusser Z, Rancz EA, Freund TF, Mody I. Cell type- and synapse-specific variability in synaptic GABAA receptor occupancy. The European journal of neuroscience 2000;12:810–818. [PubMed: 10762310]

Hegedus B, Dasgupta B, Shin JE, Emnett RJ, Hart-Mahon EK, Elghazi L, Bernal-Mizrachi E, Gutmann DH. Neurofibromatosis-1 regulates neuronal and glial cell differentiation from neuroglial progenitors in vivo by both cAMP- and Ras-dependent mechanisms. Cell Stem Cell 2007;1:443–457. [PubMed: 18371380]

Introini-Collison IB, Castellano C, McGaugh JL. Interaction of GABAergic and [beta]-noradrenergic drugs in the regulation of memory storage. Behavioral and Neural Biology 1994;61:150–155. [PubMed: 8204080]

Kelleher RJ 3rd, Govindarajan A, Jung HY, Kang H, Tonegawa S. Translational control by MAPK signaling in long-term synaptic plasticity and memory. Cell 2004;116:467–479. [PubMed: 15016380]

Kim JJ, Fanselow MS. Modality-specific retrograde amnesia of fear. Science 1992;256:675–677. [PubMed: 1585183]

Kleschevnikov AM, Belichenko PV, Villar AJ, Epstein CJ, Malenka RC, Mobley WC. Hippocampal Long-Term Potentiation Suppressed by Increased Inhibition in the Ts65Dn Mouse, a Genetic Model of Down Syndrome. J Neurosci 2004;24:8153–8160. [PubMed: 15371516]

Kushner SA, Elgersma Y, Murphy GG, Jaarsma D, van Woerden GM, Hojjati MR, Cui Y, LeBoutillier JC, Marrone DF, Choi ES, et al. Modulation of presynaptic plasticity and learning by the H-ras/extracellular signal-regulated kinase/synapsin I signaling pathway. J Neurosci 2005;25:9721–9734. [PubMed: 16237176]

Li W, Cui Y, Kushner SA, Brown RAM, Jentsch JD, Frankland PW, Cannon TD, Silva AJ. The HMG-CoA Reductase Inhibitor Lovastatin Reverses the Learning and Attention Deficits in a Mouse Model of Neurofibromatosis Type 1. Current Biology 2005;15:1961–1967. [PubMed: 16271875]

Lindner MD. Reliability, Distribution, and Validity of Age-Related Cognitive Deficits in the Morris Water Maze. Neurobiology of Learning and Memory 1997;68:203–220. [PubMed: 9398584]

Lynch TM, Gutmann DH. Neurofibromatosis 1. Neurol Clin 2002;20:841–865. [PubMed: 12432832]

Martin GA, Viskoohil D, Bollag G, McCabe PC, Crosier WJ, Haubruck H, Conroy L, Clark R, O'Connell P, Cawthon RM. The GAP-related domain of the neurofibromatosis type 1 gene product interacts with ras p21. Cell 1990;63:843. [PubMed: 2121370]

McElroy MW, Korol DL. Intrahippocampal muscimol shifts learning strategy in gonadally intact young adult female rats. Learn Mem 2005;12:150–158. [PubMed: 15805313]

Morris RGM, Garrud P, Rawlins JNP, O'Keefe J. Place navigation impaired in rats with hippocampal lesions. Nature 1982;297:681–683. [PubMed: 7088155]

Nitz D, McNaughton B. Differential modulation of CA1 and dentate gyrus interneurons during exploration of novel environments. J Neurophysiol 2004;91:863–872. [PubMed: 14523073]

North K. Neurofibromatosis type 1. American journal of medical genetics 2000;97:119–127. [PubMed: 11180219]

Rueda N, Florez J, Martinez-Cue C. Chronic pentylenetetrazole but not donepezil treatment rescues spatial cognition in Ts65Dn mice, a model for Down syndrome. Neurosci Lett 2008;433:22–27. [PubMed: 18226451]

Selcher, JC.; Atkins, CM.; Trzaskos, JM.; Paylor, R.; Sweatt, JD. Learning & memory. Vol. 6. Cold Spring Harbor, NY: 1999. A necessity for MAP kinase activation in mammalian spatial learning; p. 478-490.

Silva AJ, Frankland PW, Marowitz Z, Friedman E, Lazlo G, Cioffi D, Jacks T, Bourtchuladze R. A mouse model for the learning and memory deficits associated with neurofibromatosis type I. Nature Genetics 1997;15:281–284. [PubMed: 9054942]

Stenman J, Toresson H, Campbell K. Identification of two distinct progenitor populations in the lateral ganglionic eminence: implications for striatal and factory bulb neurogenesis. J Neurosci 2003;23:167–174. [PubMed: 12514213]

Sweatt JD. Mitogen-activated protein kinases in synaptic plasticity and memory. Current opinion in neurobiology 2004;14:311–317. [PubMed: 15194111]

Wiltgen BJ, Sanders MJ, Ferguson C, Homanics GE, Fanselow MS. Trace fear conditioning is enhanced in mice lacking the {delta} subunit of the GABAA receptor. Learn Mem 2005;12:327–333. [PubMed: 15897254]

Xu GF, O'Connell P, Viskochil D, Cawthon R, Robertson M, Culver M, Dunn D, Stevens J, Gesteland R, White R, et al. The neurofibromatosis type 1 gene encodes a protein related to GAP. Cell 1990;62:599–608. [PubMed: 2116237]

Zhu Y, Romero MI, Ghosh P, Ye Z, Charnay P, Rushing EJ, Marth JD, Parada LF. Ablation of NF1 function in neurons induces abnormal development of cerebral cortex and reactive gliosis in the brain. Genes & development 2001;15:859–876. [PubMed: 11297510]

Zhuo L, Theis M, Alvarez-Maya I, Brenner M, Willecke K, Messing A. hGFAP-cre transgenic mice for manipulation of glial and neuronal function in vivo. Genesis 2001;31:85–94. [PubMed: 11668683]

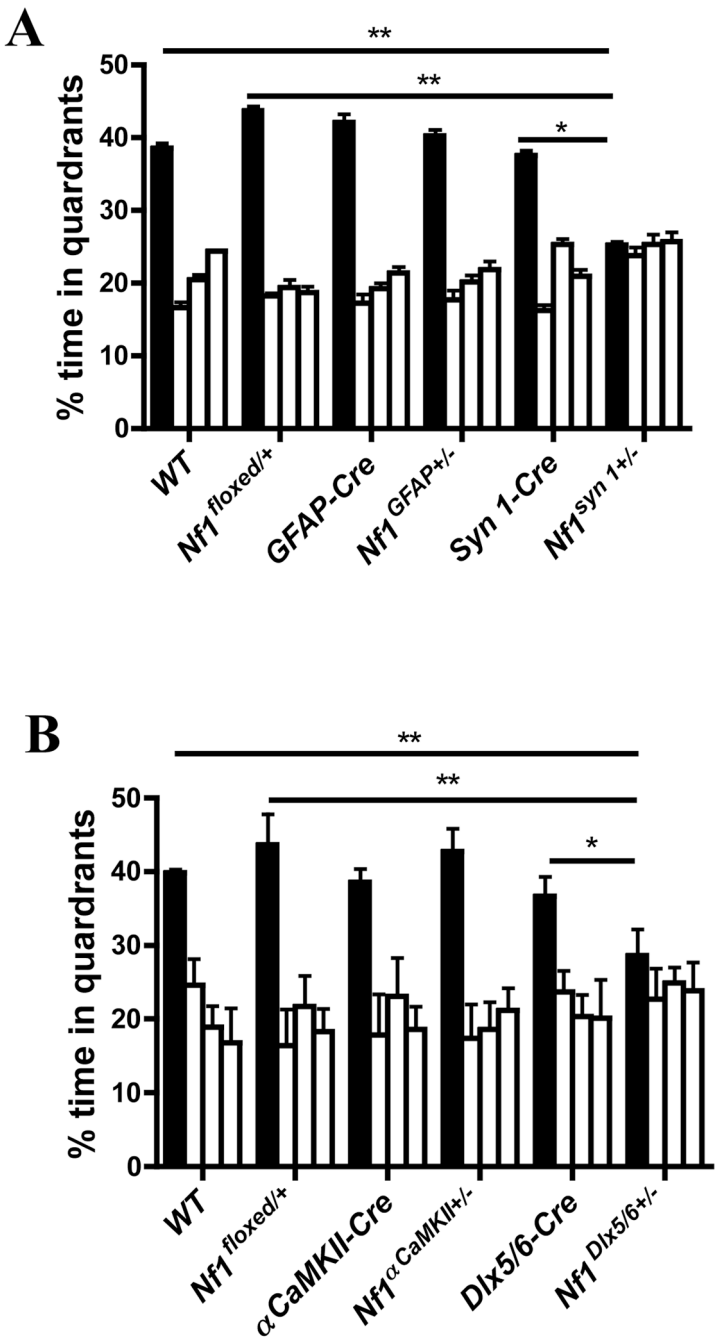

Figure 1. Cre-deletions of neurofibromin gene in inhibitory neurons cause learning deficits

A. $Nf1^{syn\ I+/-}$ (n=13), $Nf1^{GFAP+/-}$ (n=12) and their littermates controls (WT, n=16; $Nf1^{floxed/+}$, n=15; *syn I-cre*, n=14 and *GFAP-Cre*, n=11) were trained with 2 trails per day in the Morris water maze. A probe trial conducted after 7 days of training revealed that $Nf1^{syn\ I+/-}$ mice showed no preference for the target quadrant, but $Nf1^{GFAP+/-}$ mice and their littermates did ($F_{(3, 48)}$ =0.045, p=0.987 and $F_{(3, 41)}$ =7.873, p<0.001 for $Nf1^{syn\ I+/-}$ and the $Nf1^{GFAP+/-}$ mice, respectively; one-way ANOVA). Since the $Nf1^{syn\ I+/-}$ and $Nf1^{GFAP+/-}$ are in the same genetic background, the same group of WT and $Nf1^{floxed/+}$ mice (including littermates of $Nf1^{synI+/-}$ and $Nf1^{GFAP+/-}$ mice) were used as controls. **B.** The distribution of target quadrant occupancy during the day 7 probe trial showed that $Nf1^{Dlx5/6+/-}$ (n=8) had no

preference for the target quadrant, but $Nf1^{\alpha CaMKII+/-}$ (n=8) and their littermate controls (WT, n=8; $Nf1^{floxed/+}$, n=7; *Dlx5/6-cre*, n=7; and *αCaMKII-Cre*, n=8) searched selectively in the target quadrant($F_{(3, 28)}$ =12.102, p<0.001 and $F_{(3, 28)}$ =0.458, p=0.7141; for $Nf1^{\alpha CaMKII+/-}$ and the $Nf1^{Dlx5/6+/-}$ mice, respectively; one-way ANOVA). The same WT and $Nf1^{floxed/+}$ mice were used as controls because $Nf1^{Dlx5/6+/-}$ and $Nf1^{\alpha CaMKII+/-}$ mutations were on the same genetic background. The figure shows % search times for each of the four quadrants: target (in black), adjacent left, opposite, and adjacent right quadrants (in that order). All statistical comparisons are presented in Table S2 and Table S3.

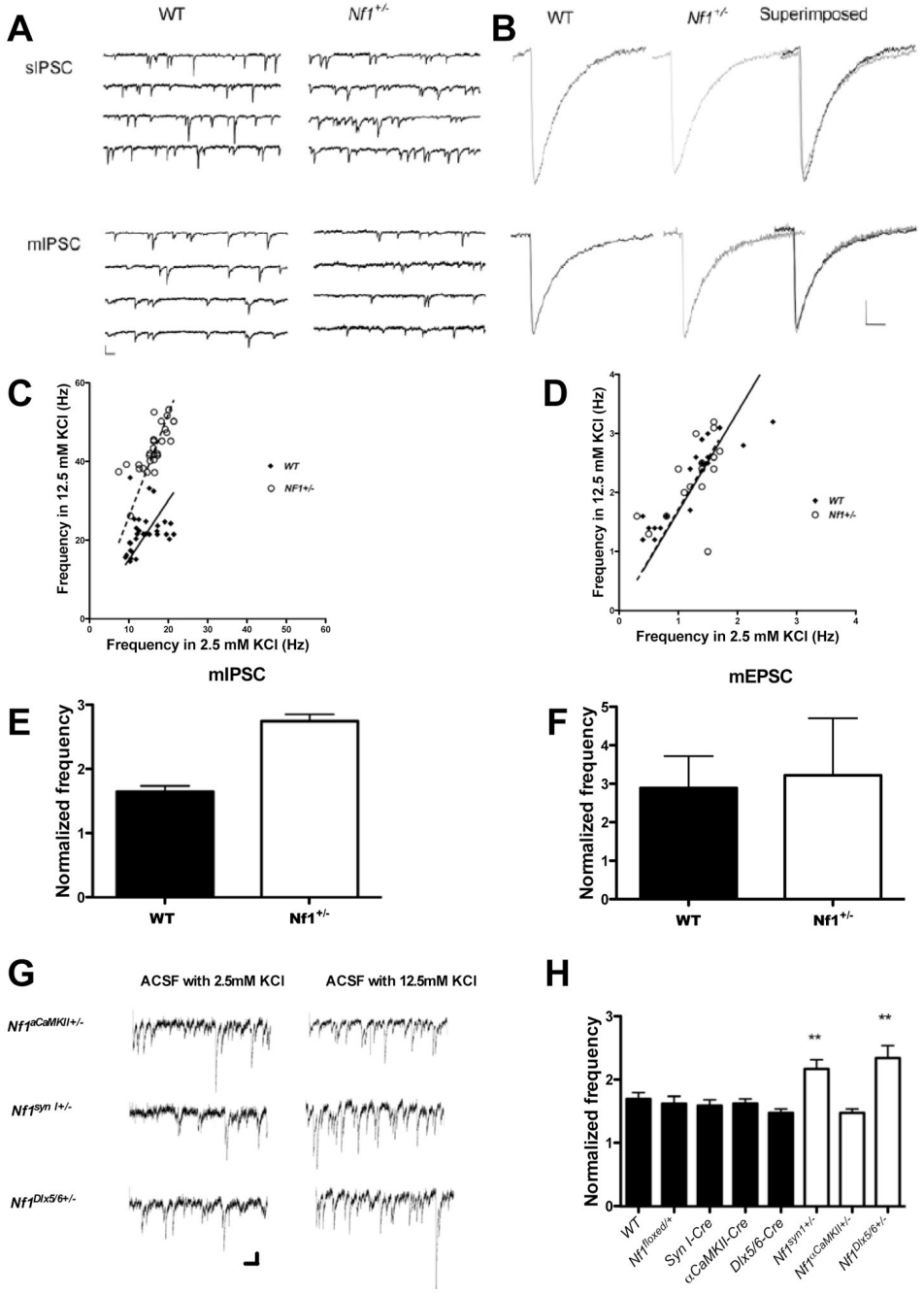

Figure 2. Increased mIPSC frequency in $Nf1^{+/-}$; mutants in high KCl

A. Representative traces of sIPSCs and mIPSCc recorded from CA1 pyramidal neurons of WT and $Nf1^{+/-}$ mice with normal ACSF (2.5mM KCl). Calibration: 100 pA, 100 ms; **B.** Average of more than 100 events of sIPSCs or mIPSCs from WT or $Nf1^{+/-}$ neurons. Calibration: 50 ms and 10pA. **C** and **D**: Frequency of mIPSC(e) and mEPSCs(f) recorded in normal and high K + ACSF. The individual points represent recordings from different neurons. Solid black squares represent WT and open squares represent $Nf1^{+/-}$ neurons. Solid lines (WT) and dashed lines ($Nf1^{+/-}$) represent the change ratio of the mIPSC or mEPSC frequency of neurons in 12.5 mM KCl versus 2.5 mM KCl ACSF. **E** and **F**. Comparison of normalized mIPSC (**C**) frequencies and mEPSC (**D**) in WT and $Nf1^{+/-}$; Data are presented as mean ± SEM. **C.** High KCl (12.5

mM) in ACSF resulted in a significant increase in mIPSC frequency in both WT and $Nf1^{+/-}$ mice (WT: 13.89 ±0.69Hz vs. 21.98±0.95 Hz, n=30, paired t-test, t=8.306, P<0.001; $Nf1^{+/-}$: 16.26±0.65Hz vs. 43.21±1.11 Hz, n=29, t=36.525, p<0.001). **E.** The ratio of mIPSC frequency recorded in high KCl to that in control solution was significantly larger in $Nf1^{+/-}$ mice (2.76 ± 0.34 n=29) than in their WT littermates (1.65 ± 0.229 n=30) (t=7.906; P<0.001). **D.** High KCl (12.5 mM) in ACSF increased the frequency of mEPSC in both WT (1.15± 0.14 Hz in normal ACSF and 2.12±0.17 in ACSF with 12.5 mM KCl, n=19, paired t-test, t=−13.585, p<0.001) and $Nf1^{+/-}$ (1.25±0.104 Hz in normal ACSF and 2.25±0.16 in ACSF with 12.5 mM KCl, n=16, paired t-test, t=−7.906, p<0.001). **F**. The ratio of mEPSC frequency recorded in 12.5 mM KCl to that in control solution was not significantly different between WT and $Nf1^{+/-}$ neurons (2.12±0.15, n=19 in WT and 2.03±0.24 n=16, in $Nf1^{+/-}$, Student's t-test, t=0.294, p=0.7708). **G** and **H**: Deletion of the *Nf1* gene from inhibitory neurons caused increased mIPSC frequency(G and H). **G**. Representative traces of mIPSCc recorded from CA1 pyramidal neurons of WT and Cre-mediated *Nf1* mutants mice with normal ACSF (2.5mM KCl) and 12.5mM KCl ACSF. Calibration: 50 pA, 100 ms; **H**. The figure shows normalized frequency changes of miniature IPSCs recorded from CA1 pyramidal neurons in 12.5 mM KCl versus 2.5 mM KCl ACSF of different *Nf1* mice with Cre-driven deletions (WT, n=20; $Nf1^{floxed/+}$, n=19; *Syn-Cre*, n=14; *αCaMKII-Cre*, n=18; *Dlx5/6-Cre*, n=13; $Nf1^{syn\ I+/-}$, n=15; $Nf1^{\alpha CaMKII+/-}$, n=15; $Nf1^{Dlx5/6+/-}$, n=14) $Nf1^{syn\ I+/-}$ and $Nf1^{Dlx5/6+/-}$, showed higher mIPSC frequencies than WT when the KCl concentration in ACSF was 12.5 mM KCl (WT: 13.52 ±0.35Hz vs. 24.31±0.71Hz; $Nf1^{syn\ I+/-}$: 15.27±0.62Hz vs. 41.26±0.37Hz; $Nf1^{Dlx5/6+/-}$: 12.46 ±0.42Hz vs. 35±0.51 Hz; the first value listed for each mutant line is for 2.5 mM and the second is for 12.5 mM KCl). In contrast, mIPSCs in $Nf1^{GFAP+/-}$ and $Nf1^{\alpha CaMKII+/-}$ mice, as well as in all controls lines, did not differ from WT mice in either normal or 12.5 mM KCl ACSF

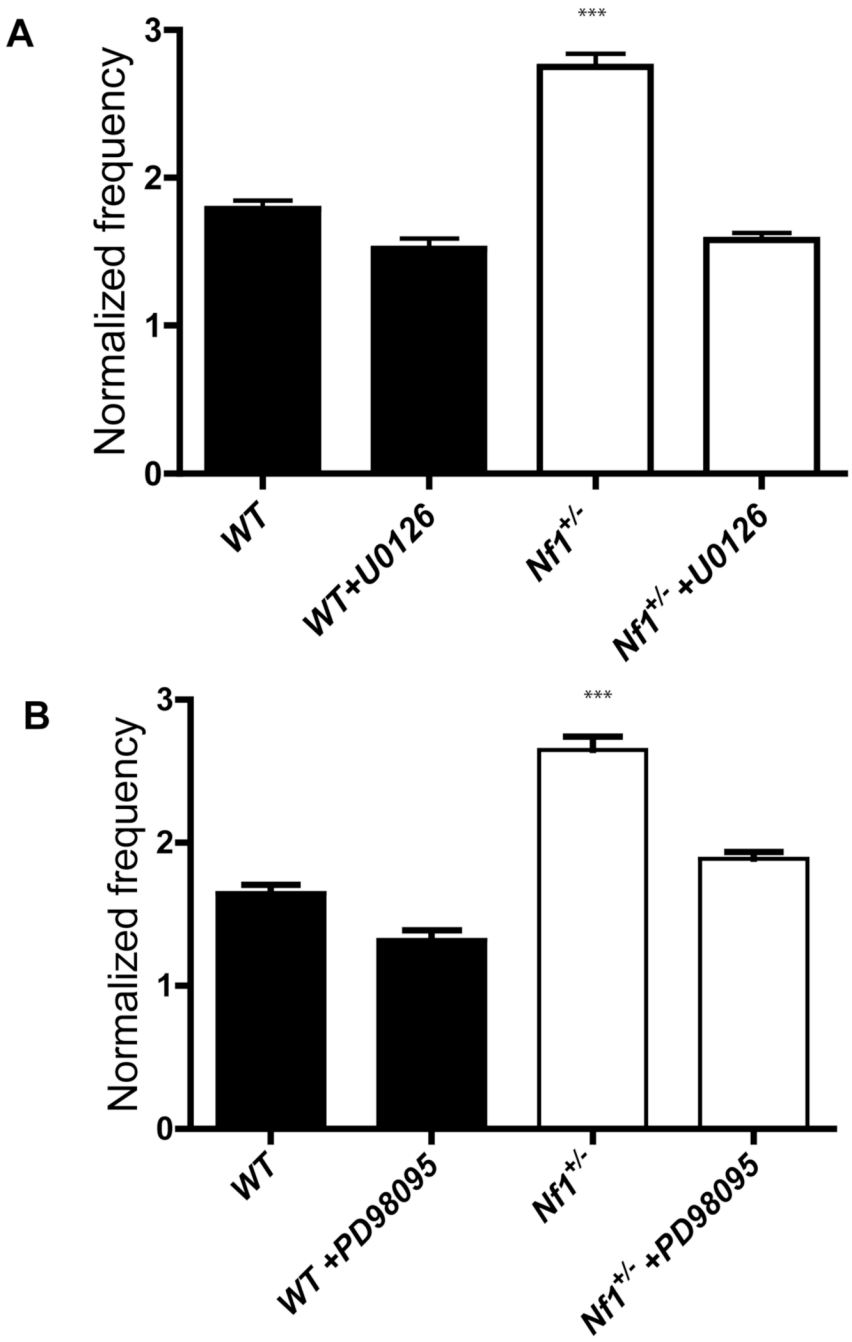

Figure 3. Increased mIPSCs frequency in *Nf1*$^{+/-}$ mice is reversed by MEK inhibitors

A. Increased mIPSCs frequency caused by high K+ ACSF perfusion is reversed by the MEK inhibitor U0126 (normalized frequency: WT w/o U0126, 1.650.058, WT w/ U0126, 1.320 ±063; *Nf1*$^{+/-}$ w/o U0126, 2.650α0.082, *Nf1*$^{+/-}$ w/ U0126, 1.89±0.067. p>0.05 for WT w/ U0126 vs. *Nf1*$^{+/-}$ w/ U0126); **B.** Increased mIPSCs frequency caused by high K+ ACSF perfusion is reversed by the MEK inhibitor PD 98095(normalized frequency: WT w/o PD98095, 1.790.057, WT w/PD98095, 1.52±0.069; *Nf1*$^{+/-}$ w/o PD98095, 2.75±0.09, *Nf1*$^{+/-}$ w/ PD98095, 1.58 ±0.047. p>0.05 for WT w/ PD98095 vs. *Nf1*$^{+/-}$ w/ PD98095).

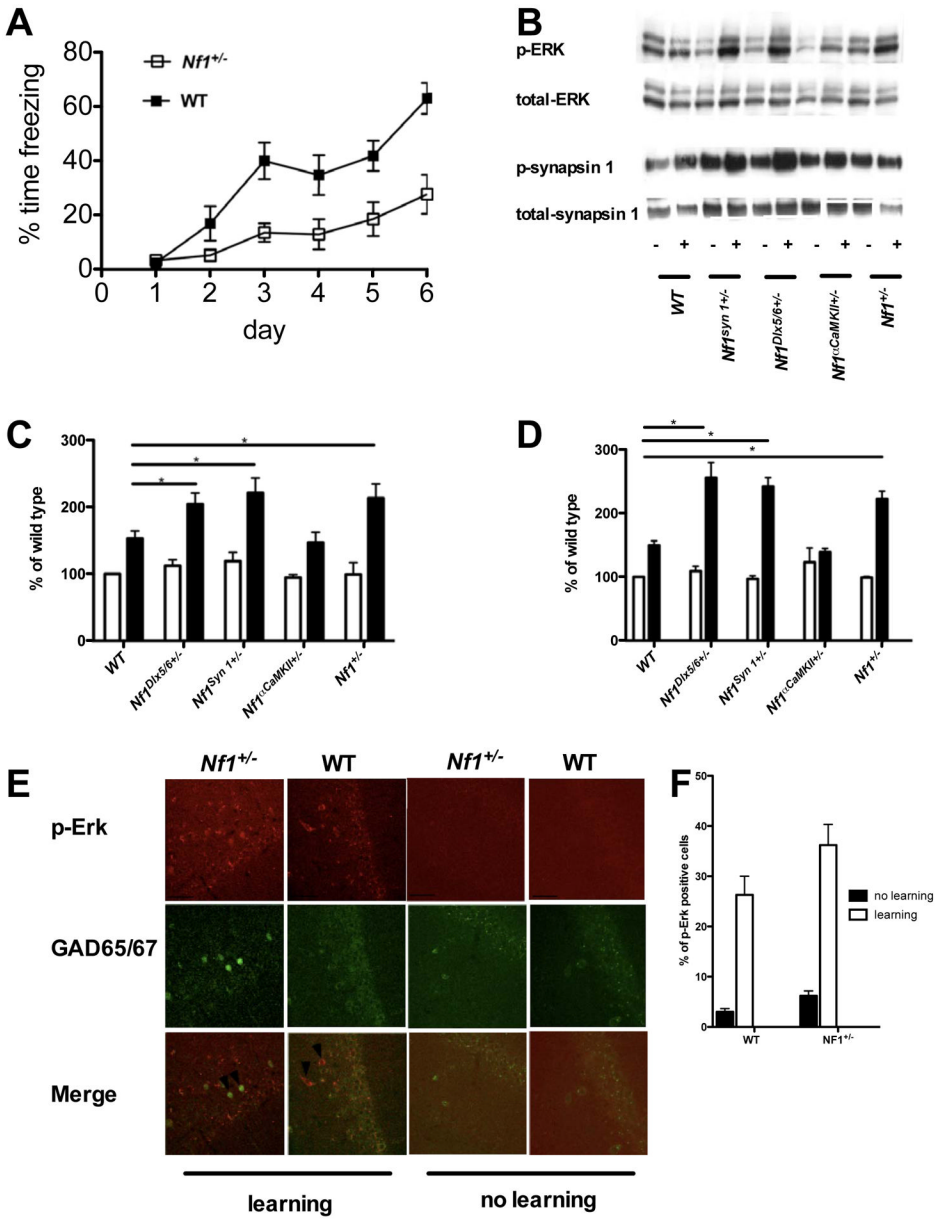

Figure 4. Increased ERK-dependent synapsin I phosphorylation in Cre-mediated Nf1 mutants

A. *Nf1*$^{+/-}$ mice have deficits in the acquisition of contextual fear conditioning *Nf1*$^{+/-}$ mice (n=16) and WT controls (n=14) were trained with a contextual fear conditioning protocol using one-trial per day for 5 consecutive days. The average freezing levels during the first 30 seconds of each training day and 24 hours after the last training trial were plotted. WT mice freeze significantly more compare to WT ($F_{(1,140)}$=3.927, P<0.05). Error bars indicate SEM. **B.** Contextual conditioning increases the phosphorylation of ERK and synapsin I (sites 4/5). Representative Western blots indicating protein bands visualized with antibodies to dually phosphorylated ERK1/2, total ERK1/2, synapsin I at sites 4/5, and total ERK1/2. + symbols denote contextual conditioning (shocks were delivered during the contextual exposure). - symbols denote that the no shock was delivered. **C** and **D**: Quantification of relative phosphorylated ERK1/2, synapsin I at sites 4/5; For each experiment, both phosphorylated and total MAPK levels were normalized to those observed in the control group of wild-type mice.

3–6 mice in each group. Values are mean ± SEM. **E**. Increased ERK phosphorylation in inhibitory neurons of *Nf1*$^{+/-}$and WT mice after Morris water maze training After spatial learning, double immunofluorescent staining shows phosphorylated ERK (Red) in inhibitory neurons (labeled with GAD65/67, Green) of both WT and *Nf1*$^{+/-}$ mice. The arrows point to examples of neurons positive for both GAD65/67 and phosphorylated ERK in the hippocampal CA1 region of WT and *Nf1*$^{+/-}$ mice. Scale bar, 50 μm. F. Quantification of the relative number of ERK phosphorylation positive inhibitory neurons in the CA1 region of *Nf1*$^{+/-}$ mutants and WT controls. The overall number of ERK phosphorylation positive inhibitory neurons in the CA1 region is higher in *Nf1*$^{+/-}$ mutant (6.2±2.2%, n=4) mice than in WT controls (3.0±1.3%, n=4, t-test, p=0.0414); after 5 training trials in the Morris water maze, the numbers of ERK phosphorylation positive inhibitory neurons in the CA1 region increased in both *Nf1*$^{+/-}$ (36.2 ±9.21%, n=5) and WT (26.3±7.43%) mice.

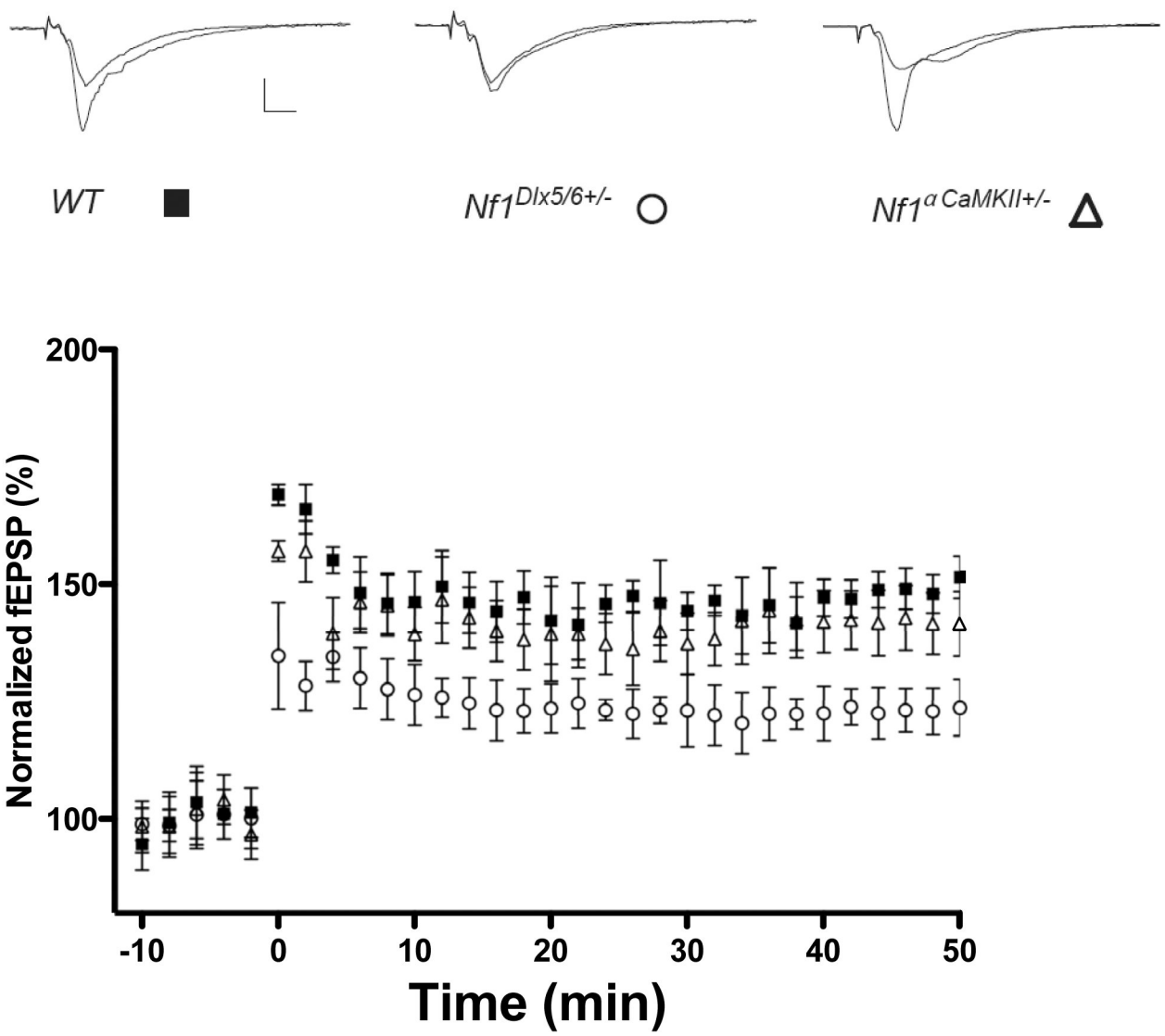

Figure 5. Impaired hippocampal CA1 LTP in *Nf1*$^{Dlx5/6+/-}$ but not *Nf1*$^{\alpha CaMKII+/-}$ mutants

LTP induced by a 5-theta-bursts tetanus (at 10 min). Each point indicates the field EPSP slope normalized to the average baseline response before the tetanus delivered at time 0. (Solid square, WT; Open circle, *Nf1*$^{Dlx5/6+/-}$ and open triangle, *Nf1*$^{\alpha CaMKII+/-}$). Between 40 and 50 min after the tetanus, the *Nf1*$^{Dlx5/6+/-}$ mice (n = 6 mice) showed 124.5% ±4.5% potentiation, the *Nf1*$^{\alpha CaMKII+/-}$ mice (n = 9 mice) showed 142.1%± 6.7% potentiation, whereas WT mice (n = 6 mice) showed 148.6% ±4.1% ($F_{(1,10)}$= 18.713, P < 0.01; $F_{(1,13)}$ =0.613, P=0.4477 for *Nf1*$^{Dlx5/6+/-}$ and *Nf1*$^{\alpha CaMKII+/-}$ respectively when compared with WT mice, one way ANOVA)

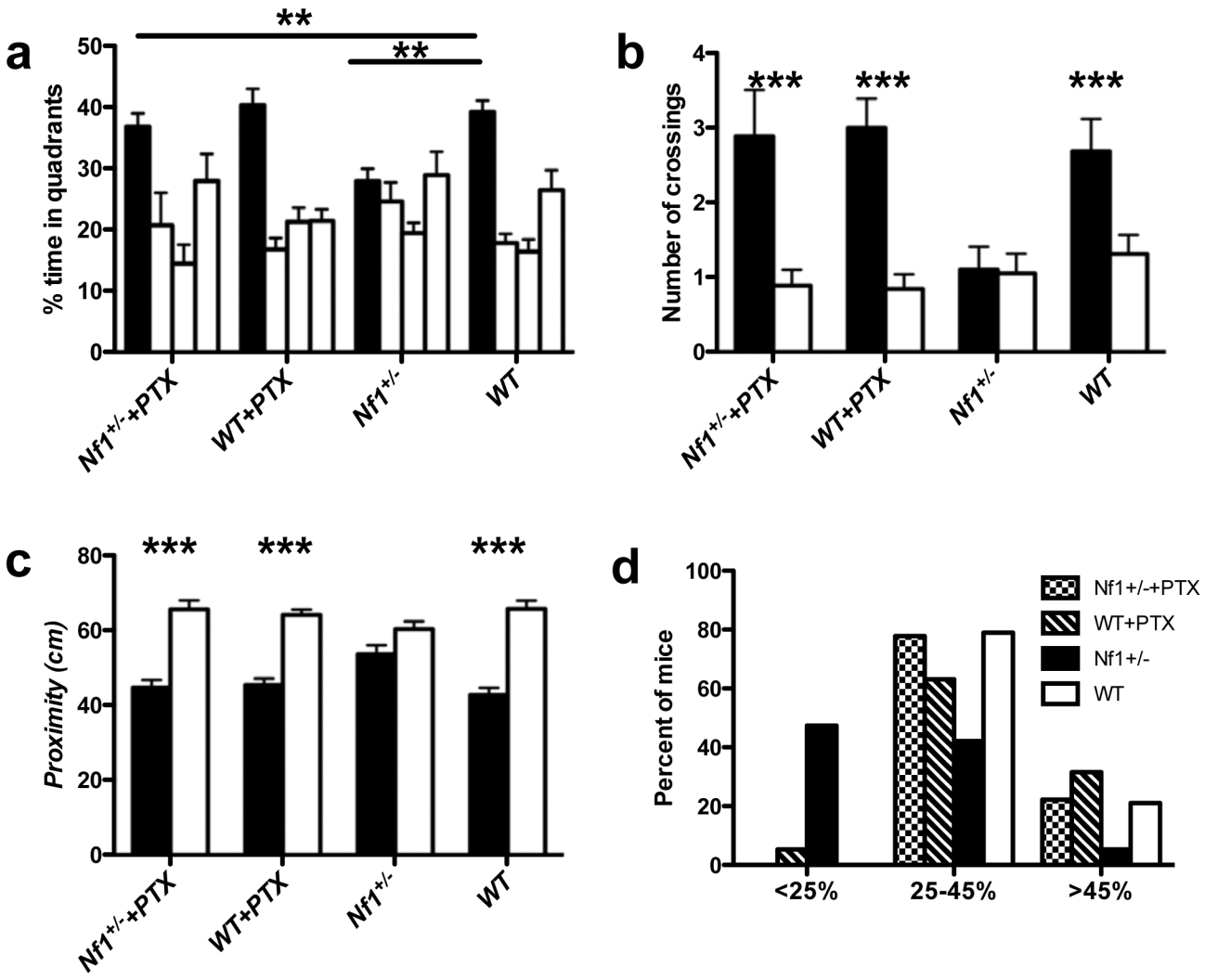

Figure 6. Spatial learning and memory deficits of *Nf1*$^{+/-}$ mice are reversed by a sub-threshold dose of picrotoxin

A. Mean percent of time spent in each quadrant during a probe trial. Analysis of the day 7 probe trial showed an interaction between genotype and treatment ($F_{(3,71)}$ = 7.937, P<0.01, two-way ANOVA). 0.01mg/Kg picrotoxin did not affect the searching time of WT mice in the target quadrant (39.23±2.20% for WT treated with saline vs. 40.40±2.64% for WT treated with picrotoxin). *Nf1*$^{+/-}$ mice treated with picrotoxin searched significantly longer in the training quadrant than *Nf1*$^{+/-}$ mice treated with saline (27.94±2.05% for *Nf1*$^{+/-}$ treated with saline vs. 36.83±2.19% for *Nf1*$^{+/-}$ treated with picrotoxin), and were indistinguishable from WT mice with or without treatment. The figure shows % search times for each of the four quadrants: target (in black), adjacent left, opposite, and adjacent right quadrants (in that order). **B**. Number of times the mice crossed the exact position where the platform was during the training (solid bar), compared with the number of crossings in the opposite position in the pool (open bar). 0.01mg/Kg picrotoxin did not affect the proximity of WT mice to the target quadrant (2.68 ±043 times for WT treated with saline vs. 3.00α0.39 for WT treated with picrotoxin). *Nf1*$^{+/-}$ mice treated with picrotoxin crossed the platform site more times than *Nf1*+/− mice treated with saline (1.11±0.30 for *Nf1*$^{+/-}$ treated with saline vs. 2.89±0.63 for *Nf1*$^{+/-}$ treated with

picrotoxin), and were indistinguishable from WT mice with or without treatment. **C**. Average proximity to the exact position where the platform was during training (solid bar), compared with proximity to the opposite position in the pool (open bar). 0.01mg/Kg picrotoxin did not affect the proximity of WT mice in the target quadrant (42.82±1.84 cm in target quadrant for WT treated with saline vs. 45.44±1.75 cm in target quadrant for WT treated with picrotoxin). *Nf1*$^{+/-}$ mice treated with picrotoxin searched significantly closer to the platform than *Nf1*$^{+/-}$ mice treated with saline (53.69±2.32 cm for *Nf1*$^{+/-}$ treated with saline vs. 44.67±2.15 cm for *Nf1*$^{+/-}$ treated with picrotoxin), and were indistinguishable from WT mice with or without treatment. **D**. Distribution of performance of each group of mice in the probe trial. The percentage of mice spending less than 25%, between 25–45% and more than 45% of the time in the training quadrant, during the day 7 probe trial, is plotted for each group. (WT, n=19; *Nf1*$^{+/-}$, n=19; WT+PTX, n=19; *Nf1*$^{+/-}$ +PTX, n=18.)

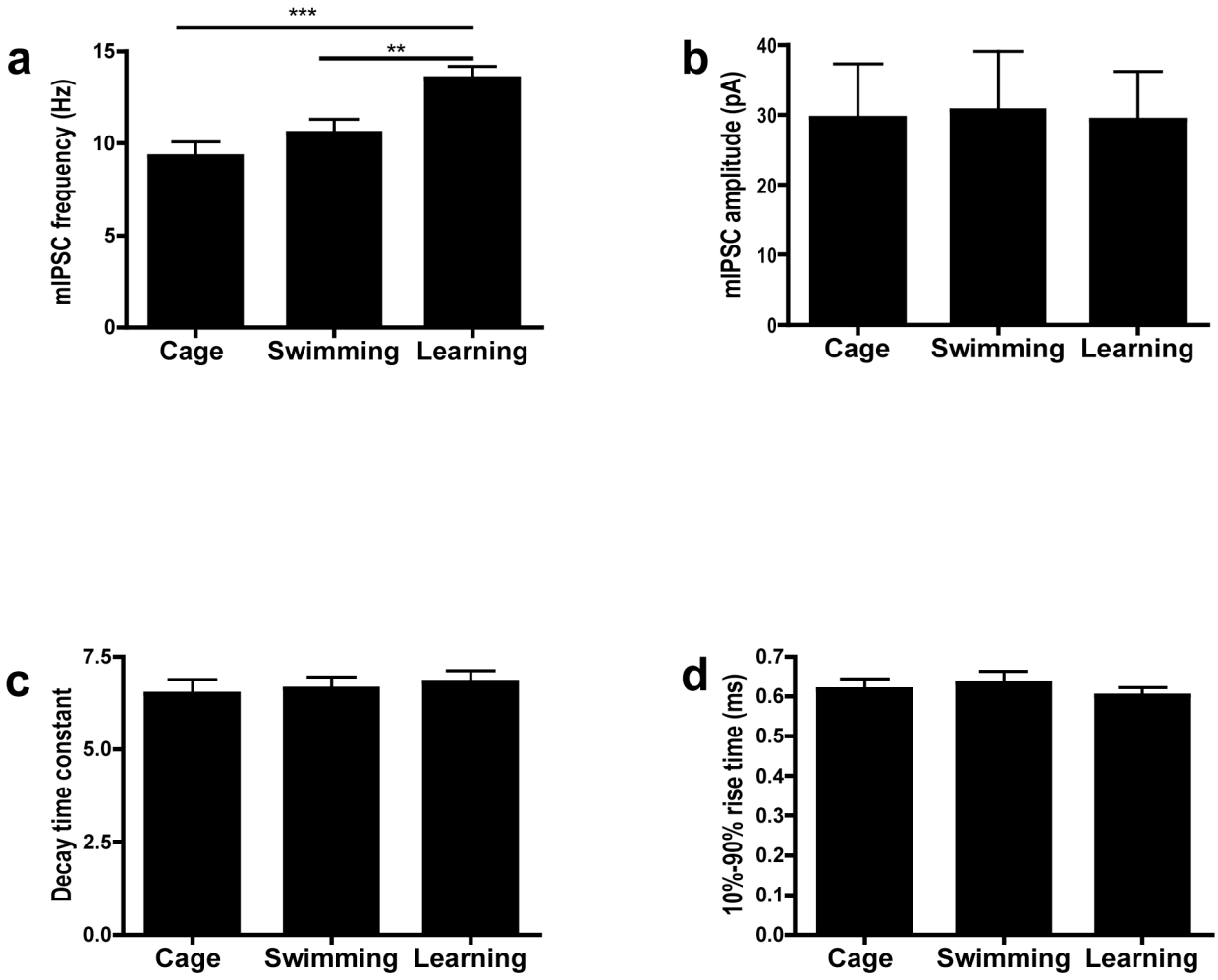

Figure 7. Spatial learning increases mIPSC frequency in hippocampal CA1 neurons

1 hr after water maze training, mIPSC frequency(**A**), amplitude(**B**), decay-time constant(**C**) and 10%–90% rise time(**D**) of the *Learning group* were compared with *Swimming control* and *Cage control* levels; (A) mIPSC frequency of the *Learning group* were significantly above control levels. ($F_{(2, 44)}$=8.954, $p < 0.001$, one way ANOVA; **P<0.01, ***P<0.001); (**B**), (**C**) and (**D**): mIPSC amplitude(b), decay time constant(c) and 10%-90% rise time(d) of the *Learning group* were not significantly different from control levels.